# Multiferroic *M*-Type Hexaferrites with a Room-Temperature Conical State and Magnetically Controllable Spin Helicity

Y. Tokunaga,[1] Y. Kaneko,[1] D. Okuyama,[2] S. Ishiwata,[3] T. Arima,[4,5] S. Wakimoto,[6] K. Kakurai,[6] Y. Taguchi,[2] and Y. Tokura[1,2,3]

[1]*Multiferroics Project, ERATO, Japan Science and Technology Agency (JST), Wako, Saitama 351-0198, Japan*
[2]*Cross-Correlated Materials Research Group (CMRG) and Correlated Electron Research Group (CERG), RIKEN, Advanced Science Institute, Wako, 351-0198, Japan*
[3]*Department of Applied Physics and Quantum-Phase Electronics Center (QPEC), University of Tokyo, Tokyo 113-8656, Japan*
[4]*Institute of Multidisciplinary Research for Advanced Materials, Tohoku University, Sendai 980-8577, Japan*
[5]*RIKEN SPring-8 Center, Hyogo 679-5148, Japan*
[6]*Quantum Beam Science Directorate, Japan Atomic Energy Agency, Tokai, Ibaraki 319-1195, Japan*

(Received 22 September 2010; published 13 December 2010)

Magnetic and magnetoelectric (ME) properties have been studied for single crystals of Sc-doped *M*-type barium hexaferrites. Magnetization ($M$) and neutron diffraction measurements revealed that by tuning Sc concentration a longitudinal conical state is stabilized up to above room temperatures. ME measurements have shown that a transverse magnetic field ($H$) can induce electric polarization ($P$) at lower temperatures and that the spin helicity is nonvolatile and endurable up to near the conical magnetic transition temperature. It was also revealed that the response (reversal or retention) of the $P$ vector upon the reversal of $M$ varies with temperature. In turn, this feature allows us to control the relation between the spin helicity and the $M$ vectors with $H$ and temperature.

DOI: 10.1103/PhysRevLett.105.257201 PACS numbers: 75.85.+t, 75.60.−d, 77.80.Dj

Mutual control of magnetization ($M$) and electric polarization ($P$) by the electric ($E$) and magnetic ($H$) fields is a major challenge in condensed-matter science and applications that may be realized by multiferroic materials. One promising example of such multiferroic materials is the spiral magnets to show the inherent $M$-$P$ coupling. Among them, the conical magnet is particularly important because they possess two magnetoelectrically controllable state variables, i.e., ferromagnetic moment and spin helicity. Among several microscopic mechanisms that can tie the magnetism with $P$, the spin current or inverse Dzyaloshinskii-Moriya model [1–3] can give the most straightforward coupling scheme irrespective of the symmetry of the underlying chemical lattice. According to this model, $P$ is expressed as

$$P \propto A \sum e_{ij} \times (S_i \times S_j) \tag{1}$$

where $A$ is a coupling constant which depends on spin exchange interaction and spin-orbit coupling, and $e_{ij}$ is the unit vector connecting neighboring spins, $S_i$ and $S_j$. What this formula means is that the interacting spins, when mutually canted, produce the local electric polarization via the spin-orbit interaction; as the additive sum of the local polarizations by every spin pair, a cycloidal (transverse helical) spin structure can generate macroscopic $P$, and the sign of the spin helicity can be controlled by means of $E$ [4,5]. Since the discovery of multiferroicity in $TbMnO_3$ [6,7], spin-cycloidal multiferroics have increasingly been found [8–14]. As the extension of the cycloidal magnet [see Fig. 1(d)], the transverse conical magnet is ferroelectric as well, as confirmed for the $CoCr_2O_4$ system [15] where magnetic reversal of $P$ was demonstrated. Although such a structure is ideal for the mutual $M$-$P$ control, transverse conical magnets are quite rare and their transition temperature ($T_{cone}$) is usually low ($T_{cone} \sim 25$ K in $CoCr_2O_4$) [15]. On the other hand, while a longitudinal conical magnet [Fig. 1(b)] has no net $P$ because of the vanishing summation of $e_{ij} \times (S_i \times S_j)$, $P$ can be readily induced by tilting the cone axis with use of $H$ [Fig. 1(c)]. One interesting class of materials to look at is the hexaferrites composed of magnetoplumbite-related members, such as $M$ type (i.e., $AFe_{12}O_{19}$: $A$ = Pb, Ca, Sr, Ba, etc.), $Y$ type (i.e., $A_2Me_2Fe_{12}O_{22}$: $Me$ = transition metal), $Z$ type (i.e., $A_3Me_2Fe_{24}O_{41}$), etc., where types of elemental blocks and their stacking order are different from each other [16]. In these materials, such a longitudinal conical structure was reported for $Y$-type hexaferrites (i.e., $Ba_2(Mg, Zn)_2Fe_{12}O_{22}$) at low temperatures ($T$) below ~50 K, where the low-$H$ control of $P$ vector becomes possible [17–22]. Although the similar $H$-induced $P$ at room temperature (RT) has been reported for polycrystalline $Z$-type hexaferrites (i.e., $Sr_3Co_2Fe_{24}O_{41}$) very recently, their magnetic structure is not yet clear [23]. The purpose of this paper is to report on the invention of the multiferroic conical states with high (near or above RT) $T_{cone}$ out of the most ubiquitous $M$-type hexaferrite magnets as well as on unique magnetoelectric control of spin chirality.

A ferrimagnetic $M$-type barium hexaferrite $BaFe_{12}O_{19}$ with the simplest crystalline structure among the

 

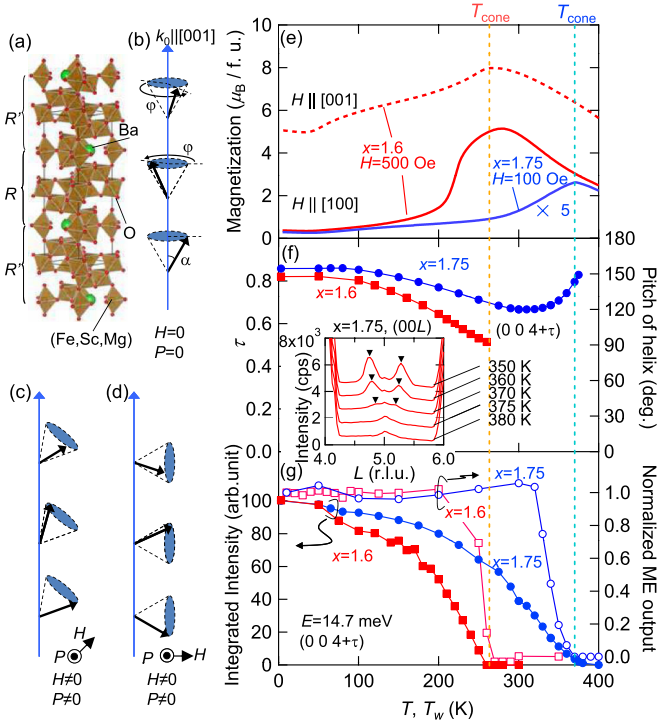


FIG. 1 (color online). (a)–(d) Schematics of (a) crystal and (b)–(d) magnetic structures of $BaFe_{12-x-\delta}Sc_xMg_\delta O_{19}$ ($\delta = 0.05$) for $T < T_{cone}$ under (b) zero, (c) tilted, and (d) transverse $H$. Black arrows represent the net moment of each spin block $R$ and $R'$. (e) Dotted (red, solid) line indicates $M$ for $x = 1.6$ in $H = 500$ Oe along the [001]([100]) direction. Solid (blue) line indicates $M$ in $H = 100$ Oe along [100] direction for $x = 1.75$ multiplied by a factor of 5. (f),(g) $T$ dependence of (f) position of the magnetic superlattice reflection at $(0\ 0\ 4 + \tau)$, calculated value of $\varphi$, (g) integrated intensity of the superlattice reflection at $(0\ 0\ 4 + \tau)$, and ME response measured at 10 K after cooling down from $T_w$. ME responses are normalized by that measured at 10 K immediately after the initial ME poling procedure (see main text). Inset shows the evolution of the magnetic superlattice peaks near $T_{cone}$ for $x = 1.75$. The residual peak on (0 0 5) at 380 K is due to the multiple scattering.

hexagonal ferrites is an industrially mass-produced uniaxial hard magnet, and the longitudinal conical structure was confirmed to emerge for partially Sc-substituted compounds $BaFe_{12-x}Sc_xO_{19}$ by neutron diffraction measurements performed at 77 K [24,25]. Therefore, the $M$-type barium hexaferrites with optimized Fe-site substitution may be a promising candidate for high-$T_C$ multiferroics with the conical spin structure. Their magnetic structure can be viewed as consisting of two blocks [$R$ and $R'$; see Fig. 1(a)] [24,25]. In the longitudinal conical phase, spins are anticipated to collinearly align within each block while the interblock coupling is noncollinear, forming a so-called "block-type" conical structure [Fig. 1(b)]. Propagation vector ($k_0$) of the helix is along the $c$ axis and the pitch of the helix ($\varphi$) and the half cone angle ($\alpha$) are 150° and 30°, respectively [24,25], in the case of $x = 1.8$.

Single crystals of $BaFe_{12-x-\delta}Sc_xMg_\delta O_{19}$ ($\delta = 0.05$) with various $x$ were grown by a floating-zone method in 10 atm $O_2$. To reduce the conductivity arising from $Fe^{2+}$ species, a small amount of Mg ($\delta = 0.05$) was added. Neutron diffraction measurements were performed using a triple-axis spectrometer TAS-1 installed at the JRR-3 of JAEA in Tokai, Japan. To measure $M$ and ME response, thin plates (with typical dimensions of $3 \times 2.5 \times 0.4$ mm$^3$) with wide faces perpendicular to the crystallographic [120] direction (with hexagonal setting) were cut from the single-crystalline rods. $P$ was measured by integrating the polarization current while sweeping $H$ with use of an electrometer (model 6517A, Keithley) and a superconducting magnet (PPMS, Quantum Design).

Figure 1(e) shows $T$ dependence of $M$ in $BaFe_{12-x-\delta}Sc_xMg_\delta O_{19}$ ($\delta = 0.05$) with $x = 1.6$ and 1.75 compounds measured along the [001] and [100] axes. The ferrimagnetic transition temperatures for these compounds are far above 400 K. For $x = 1.6$, $M$||[001] is much larger than $M$||[100], indicating the uniaxial nature of the magnetic anisotropy. As $T$ decreases, both $M$||[100] and $M$||[001] begin to decrease at around 270 K ($\equiv T_{cone}$), due to the transition from ferrimagnetic to conical spin structure. From the measurements of $M$ on a series of single-crystalline samples with different $x$, it turned out that $T_{cone}$ is maximized to 370 K at around $x = 1.75$. $T_{cone}$ was confirmed to coincide with the emergence of long-wavelength modulation of transverse spin components, indicated by $(0\ 0\ L \pm \tau)$ reflections in a neutron diffraction profile [see the inset of Fig. 1(f)]. As is shown in Figs. 1(f) and 1(g), superlattice peaks start to develop at $T_{cone}$ and their integrated intensities monotonically increase toward lower $T$. The $\varphi$ value calculated from $\tau$ monotonically increases from about 90°, then saturates at around 144° in the case of $x = 1.6$; in the case of $x = 1.75$, $\varphi$ once decreases from about 150° and starts to increase from 120° at around 300 K toward lower $T$, then saturates at around 154°. Unfortunately, rather low resistivity ($\sim 3 \times 10^7\ \Omega$ cm) of this compound prevents direct detection of the ME coupling at RT, and also makes the ME poling procedure (i.e., cooling under both $H$ and $E$ from above $T_{cone}$) difficult. Thus, we show hereafter the low-$T$ ME properties for the $x = 1.6$ compound.

Figures 2(a) and 2(b) show low-$T$ $M$-$H$ and $P$-$H$ curves for the $x = 1.6$ compound measured after ME poling. As $H$ is applied in the direction perpendicular to $k_0$ ($H$||[100]), $P$ is induced in the [120] direction, which is perpendicular to both $H$ and $k_0$ (||$c$). This result is in accord with the prediction by the spin current model expressed by Eq. (1) [1–3]. At 5 K, $P$ increases with $H$, then starts to decrease at around 5 kOe and finally vanishes above 10 kOe. At first, the cone axis gradually tilts toward the [100] direction; thus, the cycloidal component increases. This results in a monotonic increase in $P$ according to Eq. (1). As $H$ is further increased, the spin cone tends to close and $P$ starts

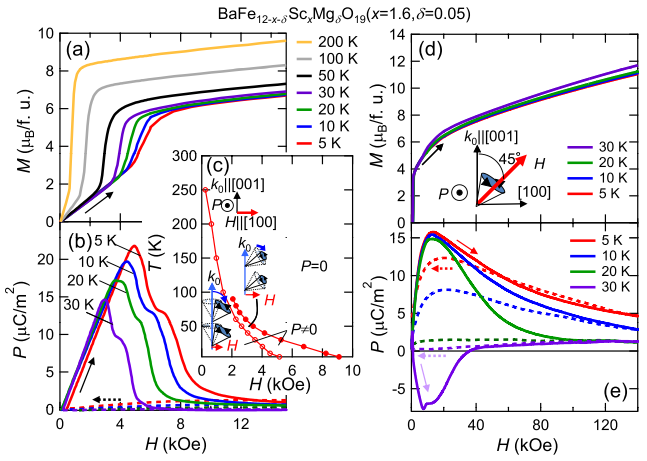


FIG. 2 (color online). (a) Initial magnetization curves measured along [100]. (b) $H$-induced $P$ measured along [120] under the application of $H$ along [100]. (c) Phase diagram obtained from the data presented in (a) and (b). Open circles represent $H$ at which $M$ shows inflection and $P$ starts to decrease, and the closed circle shows the extrapolated value at which $P$ becomes zero. The expected magnetic structure is schematically shown for each phase. (d) Initial magnetization curves measured along the tilted direction by 45° from [001] toward [100]. (e) $H$-induced $P$ measured along [120] under the application of $H$ along tilted direction from [001] toward [100] by 45°.

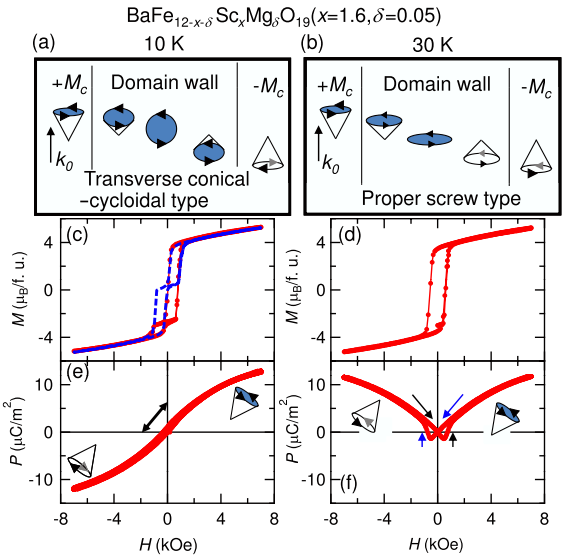


FIG. 3 (color online). (a),(b) Schema of expected domain-wall structures between positive and negative $M_c$ regions at (a) 10 K and (b) 30 K. (c),(d) $M$-$H$ curves measured at 10 K and 30 K, respectively. In (c), dashed (blue) and solid (red) lines indicate $M$ measured after zero-filed and field ($H = -250$ Oe) cooling, respectively. (e),(f) $P$-$H$ hysteresis measured along the [120] direction at (e) 10 K and (f) 30 K. In (e), the sample was initially cooled down to 10 K under the application of negative $E$ ($-3$ kV/cm) and $H$ ($-250$ Oe). Then $E$ was switched off and $H$ was swept. (f) was measured after preparing the $+P$ and $+M_c$ state.

to decrease. Then, $P$ finally vanishes due to the transition perhaps to the fanlike structure. This process is accompanied by the metamagnetic transition of first-order nature [Fig. 2(a)], and $P$ never recovers when $H$ is reduced to zero, even under the application of bias $E$. As the $T$ is increased, the transition field to the fanlike structure monotonically decreases, but the metamagnetic transition is clearly discerned even at 200 K. The resultant phase diagram is displayed in Fig. 2(c). The low-$H$ phase seems to disappear slightly above 250 K, which is almost equal to $T_{\mathrm{cone}}$. Such a low transition field suggests that the transverse conical state is not so stable in this compound as in $Y$-type hexaferrites [17–20,22], reflecting the difference in magnetic anisotropy.

Figures 2(d) and 2(e) show the $H$ dependence of $M$ and $P$ for the $x = 1.6$ compound measured after ME poling with $H$ in the tilted direction from [001] toward [100] by 45°. In contrast to the case of exactly $H \perp [001]$, the conical state appears to be robust at low $T$s in the present case, as manifested by the presence of finite $P$ even at $H =$ 140 kOe. In accord with the behavior of $P$, there is no anomaly in $M$-$H$ curves [Fig. 2(d)]. Importantly, the directions of $P$ are different between 20 K and 30 K in spite of the same ME poling and measurement procedures. This bears the important implication about the relation between the $c$-axis component of magnetization ($M_c$) and that of the spin helicity $(S_i \times S_j)_c$, as discussed below.

In Figs. 3(c)–3(f), we show $M$-$H$ and $P$-$H$ curves at 10 K and 30 K with $H$ applied in the direction tilted by 45° from the $c$ axis. Although the overall sign of $P$ depends on the ME poling procedure or history at both $T$s [26], the $P$-$H$ curves are an odd function of $H$ at 10 K, while butterfly shaped at 30 K. We attribute this difference to that of the domain wall structure of $M_c$, as depicted in Figs. 3(a) and 3(b). First, we start from the single domain state of helicity [e.g., positive $(S_i \times S_j)_c$] and $M$ (e.g., positive $M_c$) under the application of positive $H$ in the tilted direction from the $c$ axis. Suppose that $P$ is initially positive. As $H$ is decreased, the tilting angle of the cone axis monotonically decreases and vanishes at $H = 0$, at which $P$ also becomes zero. As $H$ traverses $H = 0$, the tilting angle of the cone becomes negative. Thus the $P$ changes the sign because of the sign change of the angle between the spin helicity vector and the propagation vector. Up to here, the sign of $(S_i \times S_j)_c$ is preserved. Then, $H$ reaches the coercive field and $M_c$ is reversed. At this point, how $(S_i \times S_j)_c$ behaves depends on the domain-wall structure between positive and negative $M_c$ domains. At 10 K, the domain wall appears to have a cycloidal-type (transverse conical) structure [Fig. 3(a)], and the spiral plane rotates with $M$. Thus, the sign of $(S_i \times S_j)_c$ is clamped with the sign of $M_c$, and changes as $M_c$ is reversed, similarly to the cases of $CoCr_2O_4$ [15] and $Ba_2Mg_2Fe_{12}O_{22}$ [17,19]. Then $P$ is kept to be negative upon the reversal of $M_c$. Therefore, the $P$-$H$ curve shows an odd function-like shape [27].

At 30 K, on the other hand, the domain wall between positive and negative $M_c$ is supposed to have a proper screw-type structure [Fig. 3(b)], and the half cone angle [$\alpha$; see the definition in Fig. 1(b)] increases from the positive $M_c$ side toward the domain wall (i.e., $M_c = 0$ point), and then rather decreases from 90° toward the negative $M_c$ side. In this manner, the sign of $(S_i \times S_j)_c$ is preserved across the domain wall. However, $P$ should change the sign again (i.e., from negative to positive) upon the reversal of $M_c$ because the angle between the spin helicity and the propagation vectors changes the sign here. Thus, the $P$-$H$ curve shows the butterfly shape. Now that clamping between the spin helicity and the magnetization vectors changes as $T$ varies, it is possible to control the relation between the spin helicity and the $M$ vector with $H$ and $T$ [26]. At each $T$, the $P$ value shows good retention against the repetition of $H$ reversal [26].

To study robustness of the spin helicity against the thermal agitation, ME measurements were conducted in the following way. To prepare the single domain state in terms of both spin helicity and $M$, samples were initially cooled down to 10 K under $E$ ($\sim 3$ kV/cm) along [120] and $H$ ($250 \sim 500$ Oe) along a tilted direction from the $c$ axis toward [100] by $22 \sim 45°$ from above $T_{\mathrm{cone}}$. Then, $E$ was switched off and the polarization current was measured by sweeping $H$ between $\pm 3$ kOe. After this initial measurement, the sample was warmed up to $T_{\mathrm{w}}$, then again cooled down to 10 K in the absence of $E$, while applying the bias $H$ of $250 \sim 500$ Oe to ensure the single domain state in terms of $M$. Then the ME output was measured again by sweeping $H$ at 10 K. Each ME response measured after cooling down from $T_{\mathrm{w}}$ was normalized by that measured immediately after the initial ME poling procedure. In this measurement, a reduction of the ME output signals the loss of the spin helicity. As shown in Fig. 1(g), $T_{\mathrm{w}}$ dependence of the ME output is minute up to near $T_{\mathrm{cone}}$, suggesting the robustness of the spin helicity also against thermal agitation, notably even up to 320 K for $x = 1.75$. ME output starts to decrease near $T_{\mathrm{cone}}$ and finally vanishes at around $T_{\mathrm{w}} \sim T_{\mathrm{cone}}$ due to the complete loss of the spin helicity for $T > T_{\mathrm{cone}}$.

In conclusion, the longitudinal conical spin state was confirmed for the Sc-doped $M$-type hexaferrite and its electrically fixed and magnetically controllable spin helicity (vector spin chirality) was demonstrated to be robust against magnetic-field scans as well as thermal agitations up to RT. While the rather low resistivity at around RT is an issue to be solved, $M$-type hexaferrites would be promising candidates of multiferroic materials for the RT operation of the ME control.

This work was in part supported by Grant-in-Aids for Scientific Research on Priority Areas (Grants No. 20046017 and 19052004) and the FIRST Program on "Quantum Science on Strong Correlation" from JSPS.

[1] H. Katsura, N. Nagaosa, and A. V. Balatsky, Phys. Rev. Lett. **95**, 057205 (2005).
[2] M. Mostovoy, Phys. Rev. Lett. **96**, 067601 (2006).
[3] I. A. Sergienko and E. Dagotto, Phys. Rev. B **73**, 094434 (2006).
[4] K. Shiratori *et al.*, J. Phys. Soc. Jpn. **48**, 1111 (1980).
[5] Y. Yamasaki *et al.*, Phys. Rev. Lett. **98**, 147204 (2007).
[6] T. Kimura *et al.*, Nature (London) **426**, 55 (2003).
[7] M. Kenzelmann *et al.*, Phys. Rev. Lett. **95**, 087206 (2005).
[8] S.-W. Cheong and M. Mostovoy, Nature Mater. **6**, 13 (2007).
[9] Y. Tokura and S. Seki, Adv. Mater. **22**, 1554 (2010).
[10] G. Lawes *et al.*, Phys. Rev. Lett. **95**, 087205 (2005).
[11] K. Taniguchi *et al.*, Phys. Rev. Lett. **97**, 097203 (2006).
[12] T. Kimura *et al.*, Nature Mater. **7**, 291 (2008).
[13] S. Park *et al.*, Phys. Rev. Lett. **98**, 057601 (2007).
[14] S. Seki *et al.*, Phys. Rev. Lett. **100**, 127201 (2008).
[15] Y. Yamasaki *et al.*, Phys. Rev. Lett. **96**, 207204 (2006).
[16] J. Smit and H. P. J. Wijn, *Ferrites* (Philips Technical Library, Eindhoven, 1959), p. 177–190.
[17] S. Ishiwata *et al.*, Science **319**, 1643 (2008).
[18] S. Ishiwata *et al.*, Phys. Rev. B **79**, 180408(R) (2009).
[19] K. Taniguchi *et al.*, Appl. Phys. Express **1**, 031301 (2008).
[20] S. Ishiwata *et al.*, Phys. Rev. B **81**, 174418 (2010).
[21] N. Momozawa *et al.*, J. Phys. Soc. Jpn. **54**, 771 (1985).
[22] T. Kimura, G. Lawes, and A. P. Ramirez, Phys. Rev. Lett. **94**, 137201 (2005).
[23] Y. Kitagawa *et al.*, Nature Mater. **9**, 797 (2010).
[24] O. P. Aleshko-Ozhevskii *et al.*, JETP **28**, 425 (1969).
[25] O. P. Aleshko-Ozhevskii *et al.*, JETP Lett. **7**, 158 (1968).
[26] See supplementary materials at http://link.aps.org/supplemental/10.1103/PhysRevLett.105.257201 for demonstrations of magnetic control of spin helicity and the endurance properties of $P$ against the repetition of $H$ sweeping in $BaFe_{12-x-\delta}Sc_x\ Mg_\delta O_{19}$ ($x = 1.6$, $\delta = 0.05$).
[27] Note that while the $M$-$H$ curves measured at 10 K [Fig. 3(c)] are different in shape from that measured at 30 K [Fig. 3(d)] and have a plateau at around $H = 0$, on which $M$ depends on the $H$ value at which the sample was cooled, neutron diffraction profiles along (0 0 $L$), (1 1 $L$), ($H$ $H$ 5), and (1/2 1/2 $L$) measured in the absence of $H$ do not show any notable changes between 3 K and 30 K (not shown). Therefore, this change can be ascribed not to the change of magnetic structure itself, but rather to the change of the domain wall pinning.